Vacuum xxx (2008) 1–5

Contents lists available at ScienceDirect

Vacuum

journal homepage: www.elsevier.com/locate/vacuum

Effect of thermal treatments on the structure of MoN_xO_y thin films

L. Cunha [a,*], L. Rebouta [b], F. Vaz [b], M. Staszuk [b,c], S. Malara [b,c], J. Barbosa [a], P. Carvalho [b], E. Alves [d], E. Le Bourhis [e], Ph. Goudeau [e], J.P. Rivière [e]

[a] Universidade do Minho, Departmento de Física, Campus de Gualtar, 4710-057 Braga, Portugal
[b] Universidade do Minho, Departmento de Física, Campus de Azurém, 4800-058 Guimarães, Portugal
[c] Silesian Technical University, ul. Konarskiego, Gliwice, Poland
[d] ITN, Departmento de Física, E.N.10, 2685 Sacavém, Portugal
[e] Laboratoire de Métallurgie Physique, Université de Poitiers, 86960 Futuroscope, France

Keywords:
MoN_xO_y
Structure
Annealing

A B S T R A C T

MoN_xO_y films were deposited on steel substrates by dc reactive magnetron sputtering. The depositions were carried out from a pure molybdenum target, varying the flow rate of reactive gases. X-ray diffraction (XRD) results revealed the occurrence of cubic MoN_x and hexagonal (δ-MoN) phases for the films with high nitrogen flow rates. The increase of oxygen content induces the decrease of the grain size of the molybdenum nitride crystallites. The thermal stability of a set of samples was studied in vacuum, for an annealing time of 1 h, for temperatures ranging from 500 to 800 °C in 100 °C steps. The results showed that pure molybdenum nitride films changed their structure from a meta-stable cubic MoN to hexagonal δ-MoN and cubic γ-Mo_2N-type structures with increasing annealing temperatures. The samples with molybdenum nitride films evidenced a good thermal stability, but those with molybdenum oxynitride coatings showed a tendency to detach with the increase of the annealing temperature.

1. Introduction

Metal oxynitride films represent a group of modern ceramic materials of increasing technological importance. Varying the nitrogen/oxygen ratio, we may obtain a wide range of physical properties: optical properties, obtaining a variety of different colours that may be used for decorative purposes; electrical properties, ranging from metallic (nitrides) to insulating (oxides) coatings; mechanical properties, with significant changes of the hardness; allowing these materials to provide opportunities for research and technological applications [1–8]. Molybdenum nitride thin films present interesting properties that made them a suitable material to be used as diffusion barriers [9–11] and as catalysts [12,13]. Molybdenum nitride coatings also present good tribological [14,15] and superconducting [16] properties. A variety of techniques have been used to produce polycrystalline and amorphous molybdenum nitride thin films, such as reactive magnetron sputtering [10,11,17,18], chemical vapour deposition (CVD) [9], pulsed laser deposition (PLD) [19], arc PVD [20], ion-beam deposition and ion implantation [21,22]. Molybdenum trioxide has been used as catalyst in oxidation of hydrocarbons or reduction of NO_x [23,24]. Sunu et al. studied the electrical conductivity and gas sensing properties of molybdenum trioxide [25].

Recently, transition metal oxynitrides, mainly zirconium and titanium oxynitrides, have been intensely investigated [1–8], however, the research related with molybdenum oxynitride is not so evident in the literature. There has been some investigation about molybdenum oxynitride physisorption and chemisorption [1], or as catalyst [3,4]. The studies about structural properties of this ceramic material are still rare [4,5]. The investigation of the structural arrangements of single layered molybdenum oxynitride, MoN_xO_y, is not straightforward since Mo–N systems have several stable bulk phases: face centred cubic (γ-phase), face centred tetragonal and hexagonal phase (δ-phase), strongly dependent on nitrogen partial pressure in the chamber, that add some complexity to the analysis of the structural and mechanical properties of the produced films. Molybdenum oxides may also present several stable bulk phases: m-MoO_3 (monoclinic), o-MoO_3 (orthorhombic).

In this work will be analysed the effect of thermal treatment in the stability and structure of MoN_xO_y and MoN thin films.

2. Experimental details

The MoN_xO_y and MoN films were deposited by reactive dc magnetron sputtering. The deposition system consists of two vertical rectangular magnetrons (unbalanced of type 2), in a closed field configuration. Polished high-speed steel (AISI M2)

* Corresponding author.
E-mail address: lcunha@fisica.uminho.pt (L. Cunha).

0042-207X/$ – see front matter © 2008 Elsevier Ltd. All rights reserved.
doi:10.1016/j.vacuum.2008.03.015

Table 1
Reactive gas flow during depositions, composition, thickness, deposition rate, residual stress, hardness and Young's modulus of the samples

Sample	$\phi(N_2)$ (sccm)	$\phi(O_2)$ (sccm)	Mo (at%)	N (at%)	O (at%)	t_c (μm)	Deposition rate (μm/h)	σ (GPa)	Hardness (GPa)	E (GPa)
Mo35 ($MoN_{1.08}$)	50.0	0.0	48	52	–	5.4	2.7	−1.5	25	280
Mo43 ($MoN_{1.35}O_{0.58}$)	58.5	1.5	34	46	20	3.1	3.1	−1.5	16	170
Mo41 ($MoNO_{1.19}$)	55.1	5.0	31	31	37	5.5	2.7	−1.5	20	180

and stainless steel substrates (AISI 316) were used for depositions, after ultrasonic cleaning and sputter etching for 15 min in an Ar atmosphere. Depositions were carried out using only one magnetron under an $Ar/(N_2+O_2)$ atmosphere, in static mode and the target to substrate distance was maintained constant at 70 mm. The substrate bias was also kept constant at −50 V (dc). The Ar flow was about 55 sccm in all depositions, which corresponded to a partial pressure of 0.4 Pa. The samples were prepared using a dc current density of 37.5 A m^{-2} at the molybdenum target and with a total reactive gas flux (N_2+O_2) of 60 sccm for the molybdenum oxynitride samples and 50 sccm for the molybdenum nitride sample (see Table 1). The base pressure in the deposition chamber was about 10^{-4} Pa and raised to values around 1 Pa during depositions. An external heating resistance positioned at 8 cm from the substrate holder was used to heat the samples; however, the obtained high deposition rates are probably the main cause of heating. The thermocouple position inside the chamber does not allow having an accurate value of the substrate temperature, but measurements showed that it was always higher than 250 °C. The chemical composition of the as-deposited films was determined by Rutherford backscattering spectrometry (RBS), using a 1 MeV $1H^+$ beam. RUMP code [26] was used to extract the information from the RBS spectra. An average number of five ball cratering (BC) experiments were carried out in each sample in order to determine the film thickness. The crystallographic structure was investigated by X-ray diffraction (XRD) in a conventional $\theta/2\theta$ configuration, using a monochromatic Cu Kα radiation. In order to follow structural transitions, namely peaks' positions, full width at half maximum (FWHM) and position of the peaks and grain sizes, XRD peak fitting, using Pearson VII function, was used. The coating hardness and Young's modulus were determined from the loading and unloading curves, carried out with an ultra low load-depth sensing Berkovich nanoindenter from CSM Instruments (Switzerland). A Poisson's ratio of 0.3 was used for the calculations. The maximum load used was 30 mN, with a loading time of 30 s, holding 30 s and unloading in 30 s, producing an average number of 15 indentations per sample. Film colour was computed using a commercial CM-2600d portable spectrophotometer from MINOLTA. Colour specification under the standard CIE illuminant D65 was determined and represented in the CIELAB 1976 colour space [27,28]. In order to study the thermal stability of the samples, a vacuum furnace with a base pressure of 10^{-4} Pa was used. Each sample suffered five annealing experiments, each one during 1 h at four different temperatures, ranging from 500 to 800 °C (100 °C steps). The heating rate until the desired temperature was the same for all samples and for all the annealing temperatures (around 10 °C/min). The cooling rate was not controlled ("free cooling"). After the thermal treatment at each temperature, the samples were removed from the furnace and XRD patterns, surface defects analyses and colour measurements were performed. The surface of the coatings was observed by scanning electron microscopy (SEM) and some information about composition was obtained by energy dispersive X-ray spectroscopy (EDS).

3. Results and discussion

3.1. Film deposition and characterisation

The nitrogen and oxygen contents of the as-deposited samples, extracted from RBS experiments, were normalized to the molybdenum content. The indexes of nitrogen and oxygen will be noted in the text and figures as x and y, respectively. The variation of the deposition rate, composition, structure, hardness, Young's modulus and residual stresses with reactive gas flow during deposition can be found elsewhere [5]. Table 1 shows the different deposition parameters used and some measured characteristics of the as-deposited films: composition, thickness, deposition rate, hardness and Young's modulus.

Fig. 1 shows the XRD patterns of the as-deposited samples. As discussed elsewhere [5], the structure of the sample designated in the text as $MoN_{1.08}$, reveals the formation of a molybdenum nitride phase (γ-Mo_2N, a NaCl-type structure where Mo atoms are occupying fcc sites and N atoms occupy 50% of octahedral sites (ICDD card 25-1366)) with about 52 at% of nitrogen. All the peaks present a shift to lower diffraction angles when compared to unconstrained γ-Mo_2N, and were indexed to an NaCl-type B1 cubic structure, with a lattice parameter of 0.427 nm. This meta-stable cubic MoN phase

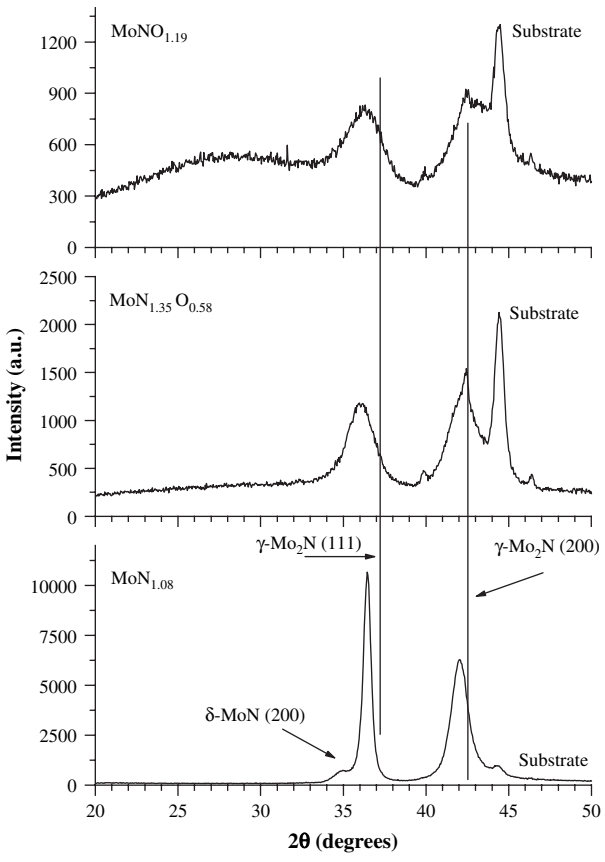

Fig. 1. XRD patterns of the as-deposited samples.

Please cite this article in press as: Cunha L et al., Effect of thermal treatments on the structure of MoN_xO_y thin films, Vacuum (2008), doi:10.1016/j.vacuum.2008.03.015

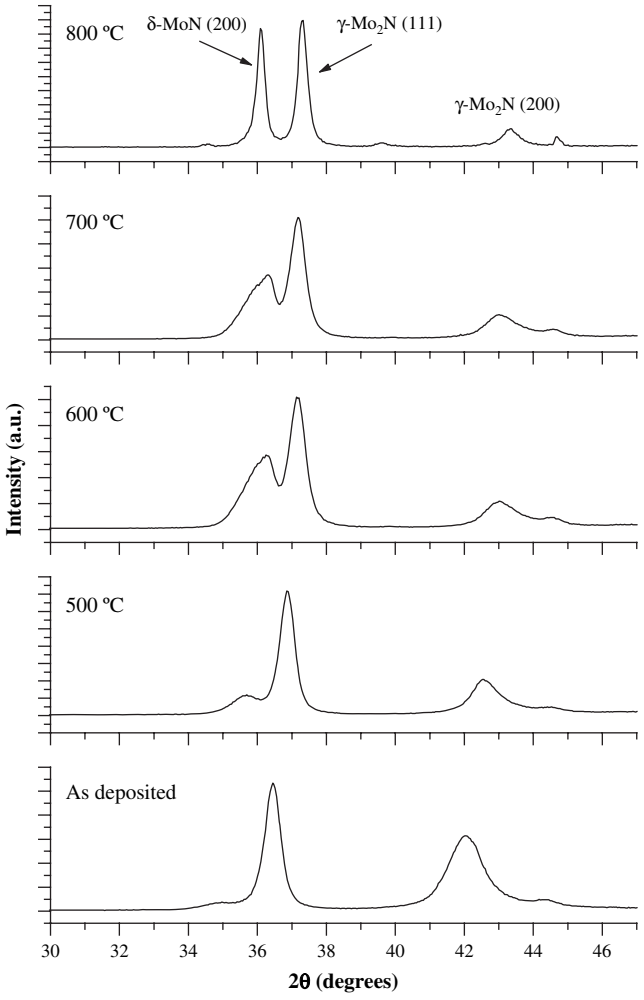

Fig. 2. XRD patterns of $MoN_{1.08}$ sample obtained after each annealing process at the indicated temperature.

has a higher lattice parameter, probably as a result of nitrogen incorporation into the fcc phase. In fact, this increase of the lattice parameter (0.419–0.427 nm) with increasing nitrogen contents (MoN_x, $0.9 < x < 1.3$) was also reported by other authors [16,29]. The 50% vacant octahedral sites of γ-Mo_2N phase may be preferentially occupied by the excess of nitrogen, but the nitrogen atoms may also occupy interstitial sites, resulting in the lattice expansion [10]. A small peak positioned at about $2\theta = 35°$, suggests also the presence of the hexagonal δ-MoN (ICCD card No. 25-1367). This hexagonal δ-MoN phase is usually formed at high nitrogen pressures, which supply the necessary high nitrogen content for this phase [20].

When oxygen is introduced into the working atmosphere, its high reactivity promotes significant changes in the as-deposited film structure [5]. The increase of oxygen content in the films composition induces a decrease of the grain size of the molybdenum nitride crystallites, as shown in Fig. 1, by the broadening of diffraction lines. The use of both oxygen and nitrogen reactive gases also induces a shift of the Bragg diffraction lines towards lower 2θ angles (meaning a higher lattice parameter (0.427 nm)), maintaining the same B1 type structure. This behavior cannot be explained by an oxide phase formation, and the nitrogen content does not justify the increase of the lattice parameter, suggesting that some oxygen is incorporated into the γ-Mo_2N phase. Part of the oxygen atoms occupies the 50% vacant octahedral sites of stoichiometric γ-Mo_2N, resulting in an expansion of the lattice [5].

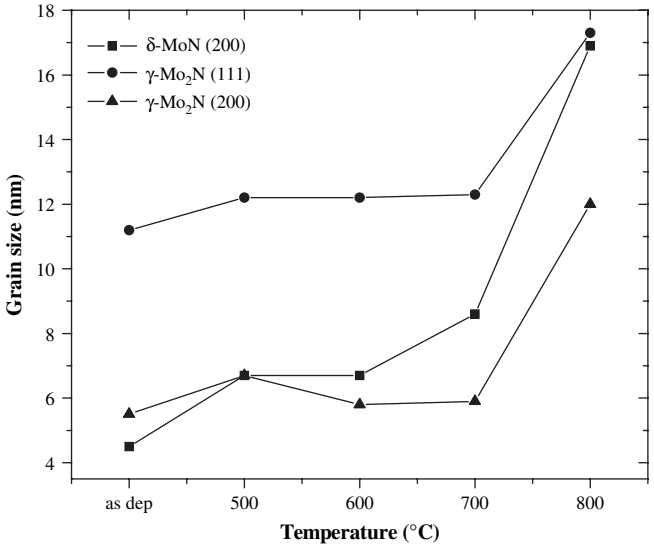

Fig. 3. Variation of the grain size of $MoN_{1.08}$ sample with the temperature of the annealing process.

The stoichiometric ratio in MoN_x compound can be higher than 1, and a x value as high as 1.7 was already reported [16]. Volpe et al. [30] and Robertson et al. [31] refer the formation of an intermediate phase: MoO_xN_{1-x}.

3.2. Thermal annealing: molybdenum nitride

For the thermal stability study, the sample with molybdenum nitride film ($MoN_{1.08}$) was used. In some aspects the results showed that the system "substrate/nitride film" has a high thermal stability. The coating didn't detach and its surface was almost unchanged during the annealing process. Anyway, detailed analysis of the XRD patterns with the annealing temperatures allowed the detection of some important structural changes (Fig. 2). The (111) diffraction

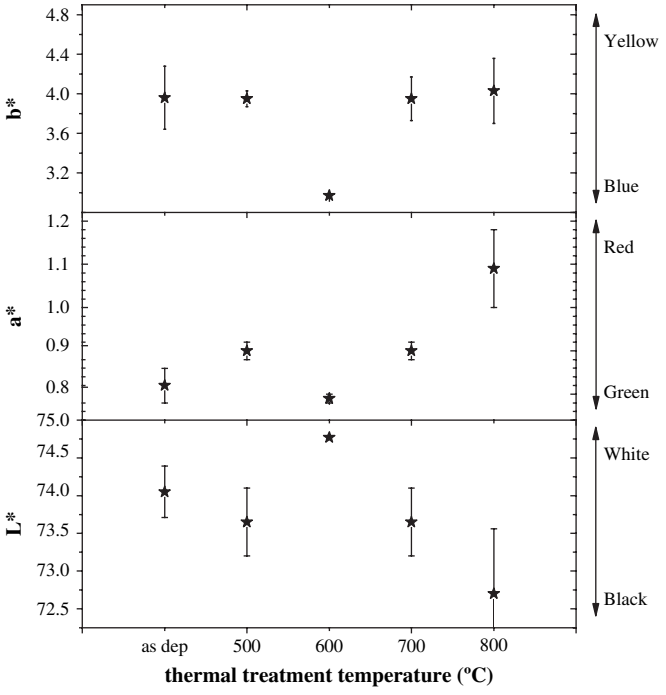

Fig. 4. Variation of L^*, a^* and b^* colour parameters of the surface of $MoN_{1.08}$ thin film with the temperature of the annealing process.

Please cite this article in press as: Cunha L et al., Effect of thermal treatments on the structure of MoN_xO_y thin films, Vacuum (2008), doi:10.1016/j.vacuum.2008.03.015

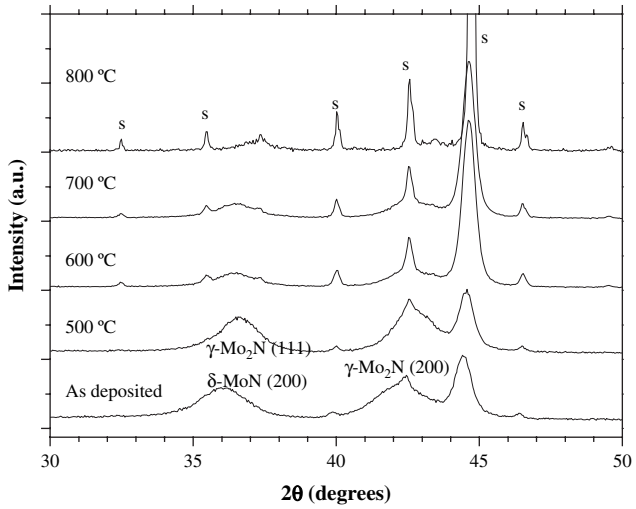

Fig. 5. XRD patterns of $MoN_{1.35}O_{0.58}$ sample obtained after each annealing process at the indicated temperature.

peak of MoN meta-stable phase detected in the as-deposited $MoN_{1.08}$ sample, shows an evident tendency to shift continuously towards the γ-Mo_2N strain free position. Simultaneously, the small peak detected at $2\theta \approx 35°$, and attributed to hexagonal δ-MoN phase, increases continuously its intensity as the thermal annealing temperature was increased. These results show that this annealing process allows the relaxation of the molybdenum nitride cubic structure from the meta-stable phase to the γ-Mo_2N phase, consequence of the segregation of nitrogen atoms. This relaxation process allows also the formation δ-MoN crystals, as evidenced in the diffraction patterns of Fig. 2. The simulation of diffraction peaks using Fourier analysis revealed an expected increase of the grain size, as shown in Fig. 3, calculated using (111) and (200) diffraction peaks of γ-Mo_2N and (200) of δ-MoN. This effect is particularly visible in the hexagonal phase, where an increase in grain size from about 4.5 nm for the as-deposited $MoN_{1.08}$ film to about 17.0 nm after the annealing at 800 °C was obtained. The results obtained using the diffraction peaks of the cubic phase were somehow difficult to analyse, revealing some constancy in grain sizes or even a small decrease after the thermal annealing from 500 to 700 °C. At 800 °C, an increase in grain size was observed. The unusual decrease (or apparent stable grain size) at intermediate temperatures might not be real since there is a change from meta-stable MoN B1 cubic structure, with most of octahedral sites occupied by nitrogen atoms (and probably some interstitial sites, too) to the stable γ-Mo_2N B1 cubic structure with only half occupation of octahedral sites. So, the apparent constancy or small decrease of grain size may be in part explained by the segregation of nitrogen atoms from the meta-stable cubic phase giving origin to the stable cubic phase and helping to increase the size of hexagonal crystals.

The thermal treatment and the detected structural changes may have consequences in the colour of the samples. Fig. 4 shows that the colour change in sample $MoN_{1.08}$ was not significant and was not perceptible to human eye. Anyway the measurements show a small decrease of lightness coordinate (L^*) and a very small change of a^* coordinate in the direction of a higher redness. The b^* coordinate is almost constant after all the annealing process.

3.3. Thermal annealing: molybdenum oxynitride

The performance of the system substrate/oxynitride films, during annealing process, was not as good as that revealed by the substrate/nitride films studied in previous section. The sample with the film with higher oxygen content ($MoNO_{1.19}$) detached completely after the thermal treatment at 500 °C, while the sample with the film with lower oxygen ($MoN_{1.35}O_{0.58}$) content revealed a slightly higher thermal resistance. The XRD patterns of this last sample after each annealing treatment is displayed in Fig. 5. It can be seen that the substrate peaks become dominant as temperature increases. The evidence of nitride phases, around $2\theta \approx 35°$, almost disappeared after the thermal treatment at 800 °C. Again the films reveal extensive detachment problems at the highest temperatures as can be evidenced from the results displayed in Fig. 6. SEM image shows what one might index as a film surface defect, but EDS spectra of the areas "*a*" and "*b*" indicate that this feature is part of the remaining coating, rich in molybdenum, while remaining bigger area corresponds to the high-speed steel substrate. In comparison to the nitride film, it is clear that the structural changes

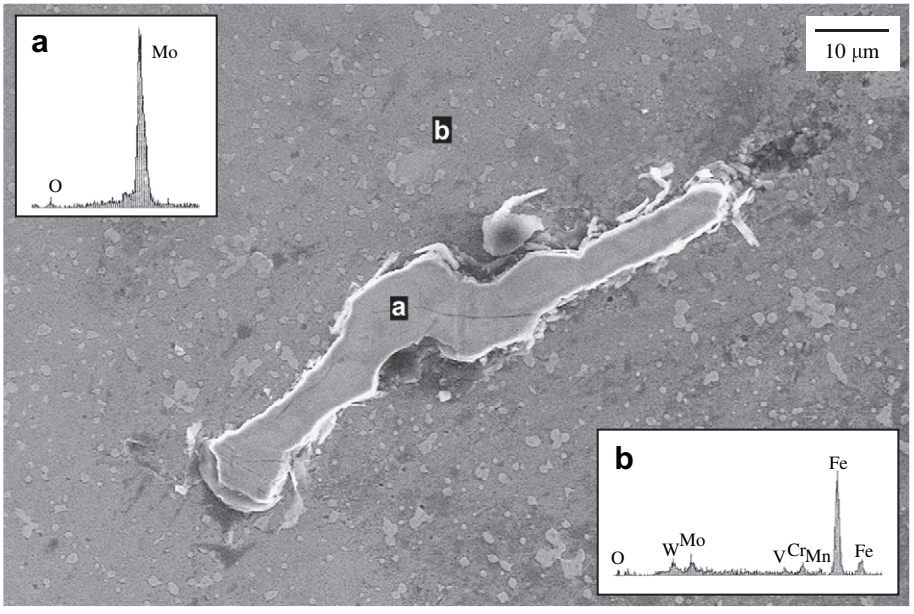

Fig. 6. SEM micrograph of the surface of the $MoN_{1.35}O_{0.58}$ sample after the thermal treatment at 800 °C. It is also observed the EDX spectra obtained in area *a* (part of remaining coating) and *b* (substrate surface).

Please cite this article in press as: Cunha L et al., Effect of thermal treatments on the structure of MoN_xO_y thin films, Vacuum (2008), doi:10.1016/j.vacuum.2008.03.015

induced by the oxygen introduction in the films structure have considerable consequences in the samples stability. The results induce the need to use other approaches if one intends to, not only understand the structural evolution with temperature, but also the possible use of these materials in "real" applications that might involve the use of these type of temperatures. The use of adhesion layers and thermally stable substrates are possibilities that should be tested in a more thorough study.

4. Conclusions

Within the limits of the temperature of the vacuum thermal treatments and of the set of samples tested in this work, the results may be summarized as follows:

- the adhesion of molybdenum nitride coating showed an higher resistance to the annealing treatments than the molybdenum oxynitride coatings. The sample with higher oxygen content detached completely after the annealing at 500 °C;
- the as-deposited molybdenum nitride thin film presented a stoichiometric meta-stable cubic structure, but the annealing process allowed the evolution to a coexistence of γ-Mo_2N B1 cubic structure with only half occupation of octahedral sites and hexagonal δ-MoN;
- the grain size of the molybdenum nitride sample increased during the annealing process. This fact is particularly noted in the crystallites of the δ-MoN phase, because in the case of cubic phase there is a change from the meta-stable cubic structure to the γ-Mo_2N structure;
- colour measurements in the molybdenum nitride film showed no significant changes with the annealing process.

Acknowledgements

The authors are grateful to the financial support of the FCT institution by the project no. POCTI/CTM/38086/2001 co-financed by European community fund FEDER.

References

[1] Sayag C, Bugli G, Havil P, Djéga-Mariadassou G. J Catal 1997;167:372.
[2] Bécue Thierry, Manoli Jean-Marie, Potvin Claude, Djéga-Mariadassou Gérald. J Catal 1997;170:123.
[3] Perez-Romo P, Potvin C, Manoli J-M, Djéga-Mariadassou G. J Catal 2002;208:187.
[4] Shen YG, Mai Yiu-Wing. Mater Sci Eng B 2002;95:222.
[5] Barbosa J, Cunha L, Rebouta L, Moura C, Vaz F, Carvalho S, et al. Thin Solid Films 2006;494:201.
[6] Carvalho P, Vaz F, Rebouta L, Cunha L, Tavares CJ, Moura C, et al. J Appl Phys 2005;98:023715.
[7] Vaz F, Cerqueira P, Rebouta L, Nascimento C, Alves E, Goudeau Ph, et al. Surf Coat Technol 2003;174–175:197.
[8] Vaz F, Cerqueira P, Rebouta L, Nascimento SMC, Alves E, Goudeau Ph, et al. Thin Solid Films 2003;447–448:449.
[9] Robertson SL, Finello D, Davies RF. Surf Coat Technol 1998;102:256.
[10] Anitha VP, Major S, Chandrashekharam D, Bhatnagar Mukesh. Surf Coat Technol 1996;79:50.
[11] Chuang Jui-Chang, Tu Shuo-Lun, Chen Mao-Chie. Thin Solid Films 1999;346:299.
[12] Li S, Lee JS. J Catal 1998;173:134.
[13] Li S, Lee JS. J Catal 1998;178:119.
[14] Ürgen M, Eryilmaz OL, Cakir AF, Kayali ES, Nilüfer B, Isik Y. Surf Coat Technol 1997;94/95:501.
[15] Kreutz KW, Krosche M, Sung H, Voss A. Surf Coat Technol 1992;53:57.
[16] Linker G, Smithey R, Meyer O. J Phys F Met Phys 1984;14:L115.
[17] Shen YG. Mater Sci Eng A 2003;359:158.
[18] Wang Yimin, Ling Ray Y. Mater Sci Eng B 2004;112:42.
[19] Bereznai M, Tóth Z, Caricato AP, Fernández M, Luches A, Majni G, et al. Thin Solid Films 2005;473:16.
[20] Kazmanli MK, Ürgen M, Cakir AF. Surf Coat Technol 2003;167:77.
[21] O'Keefe JD, Skeen CH. J Appl Phys 1973;44:4622.
[22] Fairand BP, Wilcox BA, Gallagher WJ, Williams DN. J Appl Phys 1993;64:81.
[23] Dabyburjor DB, Jewar SS, Ruckenstien E. Catal Rev Sci Eng 1979;19:293.
[24] Larrubia A, Ramis G, Busca G. Appl Catal B Environ 2000;27:L145.
[25] Sunu SS, Prabhu E, Jayaraman V, Gnanasekar KI, Seshagiri TK, Gnanasekaran T. Sens Actuator B 2004;101:161.
[26] Doolittle LR. Nucl Instrum Methods 1985;B9:344.
[27] Colorimetry. CIE Publication (Commission Internationale de L'Éclairage); 1971. 15.
[28] Recommendations on uniform color spaces, difference–difference equations, psychometric color terms, vol. 15. CIE Publication (Commission Internationale de L'Éclairage); 1978. Suppl. No. 2–70.
[29] Perry AJ, Baouchi AW, Petersen JH, Pozder SD. Surf Coat Technol 1992;54/55:261.
[30] Volpe L, Boudart M. J Solid State Chem 1985;59:332.
[31] Robertson SL, Finello D, Davis RF. Mater Sci Eng A 1998;248:198–205.

Please cite this article in press as: Cunha L et al., Effect of thermal treatments on the structure of MoN_xO_y thin films, Vacuum (2008), doi:10.1016/j.vacuum.2008.03.015